



Swansea University
Prifysgol Abertawe



Cronfa - Swansea University Open Access Repository

This is an author produced version of a paper published in :
International Journal of Fatigue

Cronfa URL for this paper:

<http://cronfa.swan.ac.uk/Record/cronfa5831>

Paper:

Whittaker, M. (2009). Effect of prestrain on the fatigue properties of Ti834. *International Journal of Fatigue*

<http://dx.doi.org/10.1016/j.ijfatigue.2009.03.008>

This article is brought to you by Swansea University. Any person downloading material is agreeing to abide by the terms of the repository licence. Authors are personally responsible for adhering to publisher restrictions or conditions. When uploading content they are required to comply with their publisher agreement and the SHERPA RoMEO database to judge whether or not it is copyright safe to add this version of the paper to this repository.

<http://www.swansea.ac.uk/iss/researchsupport/cronfa-support/>

Effect of prestrain on the fatigue properties of Ti834

MT Whittaker, WJ Evans

Swansea University

Abstract

The effects of cold dwell on titanium alloys have been widely studied in recent years, with many alloys showing detrimental mechanical properties when dwell periods are introduced at peak load. Failures in such situations are often characterised by the formation of quasi cleavage facets, and models have been suggested to explain the mechanism by which they occur. This paper seeks to investigate how different mechanical test regimes influence facet formation. It is shown in the titanium alloy Ti834 that facet formation occurs readily under stress relaxation and creep loading, but is less influenced by cyclic strain control loading. The implications of this type of strain accumulation process on the mechanical properties of Ti834 are discussed, with close correlation between suggested models and experimental data.

Keywords: Prestrain, titanium, fatigue, facets

Introduction

The near alpha titanium alloy Ti834 has exceptional high temperature creep properties up to 630°C and as such has been used in a wide variety of gas turbine applications. In developing the alloy, it was recognised that low cycle fatigue behaviour at lower temperatures is also a potential design limiting factor. An optimum compromise between high temperature creep and lower temperature fatigue was

achieved through careful control of the microstructure^[1]. In spite of this effort, it is clear that the LCF behaviour of Ti834 can be compromised by a sensitivity to dwell periods at near ambient temperatures^[2]. The sensitivity is a consequence of what has been termed ‘cold creep’ and is characterised by the development of quasi-cleavage facets on basal planes within the microstructure. As such the development of these facets is extremely dependent on microstructure.

Evans and Bache have proposed a model by which these facets develop^[3]. More recently experiments in a model large grained alloy^[4] have helped to confirm the theory that the facets form due to dislocation pile ups at the boundaries of grains unsuitably orientated for slip. The induced combination of tensile and shear components of stress leads to cleavage along the basal (or occasionally prismatic) planes resulting in what have been loosely termed ‘quasi-cleavage facets’. These microstructural features are considered highly detrimental by component designers due to the likelihood of sub surface fatigue crack initiation.

Although the mechanisms of facet formation are reasonably well understood, the specific macroscopic loading conditions under which they form is not fully understood. The number, type and orientation of facets formed shows a dependence on temperature, stress and dwell time. Indeed Sinha et al^[5] have shown that orientation of facets in Ti6242 is dependent on loading type, with the angle the facet-normal makes with the loading direction increasing in the order cyclic fatigue, dwell fatigue, static loading. The current work seeks to examine the effect of a number of different loading configurations on the development of facets in Ti834, and also the effect that varying levels of prestrain have on the mechanical properties of the alloy. Prestrain has long been utilised as a method of improving creep properties in many alloys^[6] and also in improving HCF properties in titanium^[7]. Its effects on LCF properties however, particularly under the strain control loading conditions typical of many rotating applications, have not been investigated, and may provide a mechanism of improving fatigue life.

Experimental method

A targeted programme of testing was devised in order to examine both the effect of prestrain on the mechanical properties of Ti834 and also the development of quasi-cleavage facets. Plain cylindrical specimens of nominal diameter 5.5mm were utilised, with exact measurements taken using a micrometer before each test. Three levels of prestrain were applied to the batch of specimens, with one set of specimens tested in the as received condition. This allowed for four testing conditions:-

- i) As received, or 0% prestrain
- ii) 2% tensile prestrain
- iii) 8% tensile prestrain
- iv) 2% compressive prestrain or -2% prestrain

The prestrains quoted are in terms of total applied strain, and therefore contain elastic and plastic components, the elastic part of which is recovered on unloading (usually about 0.75%). The strain was applied at a constant strain rate of 0.5%/sec using an MTS extensometer with a gauge length of 12mm.

Specimens from each prestrain batch were then tested under the following conditions:-

- i) Strain control fatigue at 20°C under R=-1 conditions with a peak strain of 1% at a constant strain rate of 0.5%/sec until failure (Classed as a 10% drop in load from the stabilised condition) using a trapezoidal 1-1-1-1 waveform, according to BS7270^[8]
- ii) Stress relaxation at 20°C for 3 hours at a constant strain of 1%. These specimens were then cycled to failure under the same conditions used in (i)
- iii) Ambient temperature (20°C) creep testing at 950MPa and under constant load conditions

Results

The IMI834 (Ti834) was supplied in the form of bar stock and had a bimodal microstructure, Figure 1, containing primary α grains of varying shapes and sizes, ranging from 20-200 μm in maximum length. Figure 2 shows a higher magnification image of the microstructure where Widmanstätten lathes of 2 - 5 μm in thickness and 20 - 50 μm in length are evident.

After the initial prestraining specimens were unloaded and removed from the machine. The resultant stress-strain curves for the -2% (2% compressive) and 8% prestrains are shown in Figures 3 and 4.

Modulus values of 114-129 GPa were measured during prestraining, consistent with the published average value of 120GPa on the TIMET website^[9].

Stress relaxation tests

The effects of prestrain on stress relaxation of the material are recorded in Figure 5. The greatest tensile prestrain displays the least stress relaxation, both as a percentage drop in stress over the 3 hours, and as a final stress. The final stresses of the specimens are ordered in terms of tensile prestrain with the 8% prestrain specimen highest, followed by the 2% prestrain, and the 0% prestrain, with the -2% prestrain achieving the lowest final stress.

Figure 6 however shows that this is also a consequence of the conditions achieved on loading. The 2% prestrain test attained the highest stress, but then relaxed significantly to achieve a lower final stress than the 8% prestrain specimen. It is clear that the greatest effect of the prestrain is on the yield stress, which differs considerably between the different levels. Thus in the -2% prestrain specimen it is difficult to obtain a true modulus from the loading curve because the material begins to yield at approximately 400MPa, whereas in the 2% prestrain specimen, yield is at 1000MPa approximately.

Strain control tests

Two types of loading sequence were used in the strain control tests. In the first, the specimen was initially loaded to a 1% tensile strain prior to strain control cycling at $R=-1$ (Tension-Compression, or T-C). For the second the specimen was first loaded into compression before commencing the $R=-1$ strain control cycle (Compression-Tension, or C-T). Two specimens of each prestrain level were tested, one tension first and the other compression first. The resultant lives are recorded in Table 1, along with values for the maximum stress, minimum stress and stress range at the stabilised condition. Additional data are recorded in Table 2 for specimens that had previously experienced stress relaxation for three hours, and then subsequently been subjected to strain control cycling to failure at $R=-1$ and a 1% peak strain (tension first).

The first loops for the different prestrains (of non-stress relaxed specimens) provide a clearer indication of the effects of prestrain, Figure 7. The tensile parts of the loops match the loading curves for the stress relaxation tests. Clear differences however can be observed from the compressive part of the cycle. Firstly the prestrain causes a drop in yield stress in the opposite quadrant of the stress-strain loop, i.e. tensile prestrains reduce the compressive yield stress, and the compressive prestrains reduce the tensile yield stress. Secondly it is noticeable from Table 1 that the different prestrains result in different values for the stabilised stress range ($\Delta\sigma$) at half life. The highest $\Delta\sigma$ occurs in the 0% prestrain specimens and the lowest in 8% prestrain tests.

Figure 8 shows the evolution of maximum and minimum stress throughout each test. It is clear that despite the initial prestrain, and the change in the shape of the initial loops, each test tends towards a common maximum stress. This is not the case with the minimum stress. Similar results are evident from the maximum stress of the 'compression first' tests shown in Figure 9, although the minimum stress values, with the exception of the 8% prestrain test, now approach a consistent value.

Discussion

Ti834 was selected for this investigation because of its well established tendency to show time dependent effects at ambient temperatures. Previous work^[10, 11] has shown that this 'cold creep' is characterised by the formation of quasi-cleavage facets, and a mechanism for their formation has been proposed by Evans and Bache, based on the offloading of stress from suitably orientated 'weak' grains onto neighbouring 'hard grains'. The resultant combination of tensile and shear stresses allows for cleavage of grains, often orientated with basal planes near perpendicular to the loading direction. Recent work by Sackett et al^[4] however has shown that in the absence of suitably orientated basal grains, cleavage of prismatic orientated grains may occur.

In the present work faceting was evident in the specimens that had undergone stress relaxation. Previous work^[12] has shown that in a similar titanium alloy, Ti6-4, the formation of facets is indeed a time dependent process since it was shown that no facets were formed under tensile loading, and only occurred when a period of stress relaxation was introduced.

As part of this programme, the cold creep behaviour of Ti834 was also investigated, and reported elsewhere^[10]. It is however interesting to note the effect that prestrain has on the creep properties of the material, Figure 10. It can be seen that prestrain results in a reduction in strain to failure for both -2% and 2% prestrain levels, although the rate of strain accumulation during secondary creep increased in both cases. At the larger prestrain of 8% however, the number of dislocations generated prohibits the movements of further dislocations, since thermal energies are low at room temperature, and the ability for dislocations to cross slip and climb is curtailed. These findings are consistent with the work of Odegard and Thompson^[6], who found similar results in Ti6-4, although it should be noted they were concerned with stresses lower than those used in the current tests.

It is interesting to compare the stress relaxation tests performed in the current work, with the previous creep work. Figures 5&6 highlight the variations in stress for the tests but it is perhaps more

informative to present the stress relaxation data normalised by the peak loading stress (i.e. stress at $t=0$), Figure 11. It is clear that many of the perceived differences between the -2%, 0% and 2% tests are eradicated. In each case there is a drop of 7-15% in stress over the course of 3 hours. The dislocation mechanisms controlling this reduction are similar to those responsible for strain accumulation in the creep tests, Figure 10. In the case of the 8% prestrain specimens however, a high initial dislocation density restricts further dislocation movement, thereby limiting creep strain accumulation and relaxation in stress.

The fracture surfaces of the creep specimens were characterised by extensive facetting, an example of which is shown in Figure 12, from the 0% prestrain specimen. Similar areas of facetting were observed in the stress relaxation specimens, Figure 13, although it is clear that within the creep specimens larger areas of cleavage are evident. In both cases the location of these facets is not necessarily related to the development of a crack.

It seems clear that three individual processes promote the formation of quasi cleavage facets. Fully reversed strain control fatigue at these strain levels is not one of these processes. The fact that facets do not form readily under these conditions has been demonstrated by the 0% prestrain strain control specimens. The fatigue cracks appeared to initiate at a slightly subsurface position, with a possible individual facet at the site, but other than this no facets were found. According to the Evans-Bache model the formation of these facets occurs due to the offloading of stress from a 'weak' grain orientation onto a 'strong' grain orientation. This process provides the required shear stress at grain boundaries through dislocation pile ups. However, under fully reversed strain controlled loading, it seems that these pile ups can be relaxed and do not promote extensive facetting. The most likely conclusion is that as the stress field is reversed as the specimen moves from tension to compression (or compression to tension) the pile up at the grain boundary dissipates through dislocation movement away from the boundary.

It is clear, however, that facets do form during the prestrain process. This is evident from prestrained specimens cycled to failure under strain control. Individual facets were found in all of these prestrained specimens. Since it has been shown that no facets were formed under strain control fatigue loading, by inference, the facets must have formed during the prestrain process. In this case the stress field is not reversed, and dislocation pile ups at grain boundaries are not relieved.

Indeed, examination of the fracture surfaces showed that the number of individual facets per unit area increased with prestrain level, though it is unclear as to whether the facets form during the prestrain loading, or during subsequent relaxation, or unloading. Previous work by Evans^[13] has shown how facet formation in Ti6-4 under monotonic loading occurs only when a period of stress relaxation is introduced. This work seems to indicate that it is the period of stress relaxation at peak strain, prior to unloading, that is most important in facet formation during these tests. The fact that the number of facets increased with increasing prestrain is a consequence of the higher level of plasticity achieved, consistent with findings from the creep tests at room temperature.

This argument is supported by the fact that facets formed during the stress relaxation tests, as they were found on the 0% prestrain, stress relaxed, strain control fatigued specimen. Again, since the facets do not form during the strain control fatigue process, they must have formed during the period of stress relaxation. However, facetting is limited due the decreasing stress field associated with these tests.

The most extensive facetting occurred in the 20°C creep specimens, and since evidence of this was found at the 0% prestrain level, it can be concluded that creep is a facet forming process. The fact that large areas of the fracture surface showed evidence of facetting was a reflection of the nature of the test. Unlike the stress relaxation tests, the stress across the specimen will be constant, or even increasing as facet formation occurs, reducing the volume of material. The high stress levels now easily generate adequate dislocations, which under the unidirectional stress form large areas of pile

ups, leading to cleavage. It was also noticeable that the facets encompassed not only the primary alpha grains, but also the transformation product, Figure 12.

To illustrate the reason for the larger faceted areas in the creep specimen, it is useful to consider the accumulation of plastic strain during a stress relaxation test

$$\varepsilon = \varepsilon_{el} + \varepsilon_{pl}$$

$$\varepsilon = \left(\varepsilon_{el} - \frac{\Delta\sigma}{E} \right) + \varepsilon_{pl} + \Delta\varepsilon_{pl}$$

And clearly a fixed total plastic strain is exchanged for elastic strain in the form

$$\Delta\varepsilon_{pl} = \frac{\Delta\sigma}{E}$$

Typical values of $\Delta\sigma$ are 100→150MPa giving

$$\Delta\varepsilon_p = 0.00083 \rightarrow 0.00125 = (0.083 \rightarrow 0.125)\%$$

And comparing these values to the levels of plasticity seen in the creep tests, Figure 10, it becomes clear that the significantly lower levels of plastic strain accumulated in the stress relaxation tests limit the number of facets produced. Recent work suggests^[5] these facets would most likely be orientated at approximately 70° to the axis of loading, due to the static nature of creep testing, although this has not yet been verified.

One important issue is the relationship between stress relaxation and softening that occurs during fatigue to produce the cyclic stress-strain curve. To explore this relationship the reduction in stress during the 3 hour relaxations of the prestrained samples have been superimposed on the monotonic and cyclic curves from previous R=0 repeated fatigue tests^[14], in Figure 14. The 0% prestrain test is of particular interest as it shows that the stress relaxation during the 3 hour period results in a final stress which lies on the cyclic stress-strain curve. This supports the view that cyclic relaxation is also the

result of time dependent strain accumulation. Clearly for these alloys there is a complicated interaction between low temperature fatigue and time dependent creep.

Initially it seems difficult to reconcile the 2% and 8% relaxation tests with this type of approach (assuming that the cyclic stress-strain curve mirrors the shape of the monotonic curve). However, consideration must be given to the levels of damage induced during the prestrain process. It is interesting to adopt a fracture mechanics type of approach here and consider the change in compliance during loading. A change in compliance is associated with changes in crack length but could also be evidence of increasing damage. It is interesting to note that the compliance is $7.74 \times 10^{-3} \text{GPa}^{-1}$ in the 0% specimen, $8.78 \times 10^{-3} \text{GPa}^{-1}$ following 2% prestrain and $9.52 \times 10^{-3} \text{GPa}^{-1}$ in the 8% prestrain specimen. The damage incurred in the form of facetting could account for the fact that the 2% and 8% curves fall to values below the monotonic and cyclic stress-strain curves.

Figure 15 shows the performance of the current strain control fatigue specimens, compared with previous Ti834 bar stock data tested as Swansea^[14]. It can clearly be seen that the 8% prestrain results in a significant reduction in fatigue life. The 2% prestrain test with the shorter life shows only a minor reduction in expected life, when the scatter of the data is considered. This trend is consistent with the stress relaxation tests, in that a prestrain of up to 2%, compressive or tensile, only marginally affects the mechanical properties of this alloy. For 8% prestrain however, the dislocation density produced has marked effects in terms of reduced creep rates, stress relaxation and fatigue properties.

The creep strain accumulation of the 20°C 0% specimen can be modelled by summing a logarithmic strain relationship with a linear damage criterion, $\epsilon_t = \alpha_1 \log(\alpha_2 t + 1) + \alpha_3 t$, where α_1 , α_2 , α_3 are material parameters which can be related the applied stress through a polynomial fit, Figure 16. The form of this equation indicates that accurate description of the creep curve requires both a logarithmic and linear term. The accumulation of damage can be considered to represent the development of facets throughout the test. It can be seen that the summation of the two mechanisms gives an extremely accurate representation of the creep curve. A logarithmic relationship is generally considered to be

representative of a ductility exhaustion mechanism as a strain hardening mode of deformation. The linear damage law implies that facet formation commences at the very beginning of plastic strain accumulation.

Conclusions

- Three processes examined here appear to promote the development of facets in Ti834. Individual facets form under prestrain and stress relaxation, whereas large areas of quasi-cleavage occur in creep specimens, associated with extensive plastic strain accumulation.
- At low prestrain levels of -2% and 2% the mechanical properties of the material show only minimal differences. Fatigue lives under strain control were not significantly affected and creep rates are not dramatically altered, although strain to failure is reduced. Stress relaxation on a normalized basis shows little variation.
- High dislocation densities generated by 8% prestrain does significantly alter properties. Fatigue lives are reduced as are creep rates at 950MPa at room temperature. Previous work^[6] however indicates that the prestrain effects will vary with stress in these creep tests.
- Plotting stress relaxation alongside monotonic and cyclic stress-strain curves indicates that cyclic relaxation in strain control tests may be the result of time dependent creep effects.
- The summation of a logarithmic creep term and a linear damage term to represent facet development gives an excellent representation of room temperature creep rates in this alloy.

Acknowledgements

The authors would like to thank Rolls-Royce plc for funding and technical support over the course of this work, and also the contributions of Dr Will Harrison.

References

- [1] WJ Evans and MR Bache, “Multiaxial fatigue of near alpha titanium alloys”, Eighth World Conference on Titanium, Birmingham, October 1995, Titanium `95, Eds. PA Blenkinsop, WJ Evans and HM Flower, IOM, pp. 1339–1346, 1996.
- [2] MR Bache, M Cope, HM Davies, WJ Evans, G Harrison “Dwell sensitive fatigue in a near alpha titanium alloy at ambient temperature”, International Journal of Fatigue **19** (Suppl. 1) (1997), pp. S83–S88
- [3] WJ Evans, MR Bache “Dwell and environmental aspects of fatigue in α/β titanium alloys”, Fatigue Behaviour of Titanium Alloys, The Minerals, Metals and Materials Society, 1999, pp99-110.
- [4] E.E. Sackett, L. Germain, M.R. Bache, “Crystal plasticity, fatigue crack initiation and fatigue performance of advanced titanium alloys”, International Journal of Fatigue, Volume 29, Issues 9-11, September-November 2007, Pages 2015-2021
- [5] V Sinha, MJ Mills, JC Williams, “Crystallography of fracture facets in a near alpha titanium alloy”, Metallurgical and Materials Transactions A, Vol 37A, June 2006, pp2015-2026
- [6] BC Odegard, AW Thompson “Low temperature creep of Ti-6Al-4V”, Metallurgical Transactions, Vol 5, 1974, pp1207-1213
- [7] DB Lanning, T Nicholas, GK Haritos “Effect of plastic prestrain on high cycle fatigue of Ti-6Al-4V”, Mechanics of Materials 34 (2002), pp127-134
- [8] BS7270, “British standard method for constant amplitude strain controlled fatigue testing”, British Standards Institution, 1990
- [9] Timet website, www.timet.com
- [10] MT Whittaker, WJ Evans, JP Jones, D Rugg, T Jackson “Effect of prestrain on ambient and high temperature creep in Ti834”, 11th International Conference on Titanium, Kyoto, 2007, pp 1345-1348

[11] MR Bache, M Cope, HM Davies, WJ Evans, G Harrison “Dwell sensitive fatigue in a near alpha titanium alloy at ambient temperature”, International Journal of Fatigue, 1997, pp 83-88

[12] WJ Evans “Creep-fatigue interactions in Ti-6Al-4V at ambient temperatures”, 3rd International conference on creep and Fracture of Engineering materials and structures, 1987, pp603-613

[13] WJ Evans, “Optimising mechanical properties in alpha + beta titanium alloys” Materials Science and Engineering A243 (1998) pp 89-96

[14] HM Davies, “Low temperature dwell sensitive fatigue in near-alpha titanium alloys”, PhD thesis, University of Wales Swansea, 1997

Table 1: Fatigue lives of non-stress relaxed R=-1 strain control specimens for each prestrain level

Prestrain	Loading type	Peak stress (MPa)	Minimum Stress (MPa)	Stress range (MPa)	Life
0%	Tens-Comp	938	-1018	1956	601
0%	Comp-Tens	972	-856	1828	491
2%	Tens-Comp	934	-876	1710	551
2%	Comp-Tens	933	-874	1807	681
8%	Tens-Comp	904	-745	1649	361
8%	Comp-Tens	924	-763	1687	201
-2%	Tens-Comp	847	-1001	1848	741
-2%	Comp-Tens	891	-954	1845	541

Table 2: Fatigue lives of stress relaxed specimens, cycled under R=-1 strain control conditions for each prestrain level

Prestrain	Loading type	Peak stress (MPa)	Minimum Stress (MPa)	Stress range (MPa)	Life
0%	Tens-Comp	929	-933	1862	581
2%	Tens-Comp	929	-884	1813	596

8%	Tens-Comp	926	-736	1662	301
-2%	Tens-Comp	876	-1014	1890	411

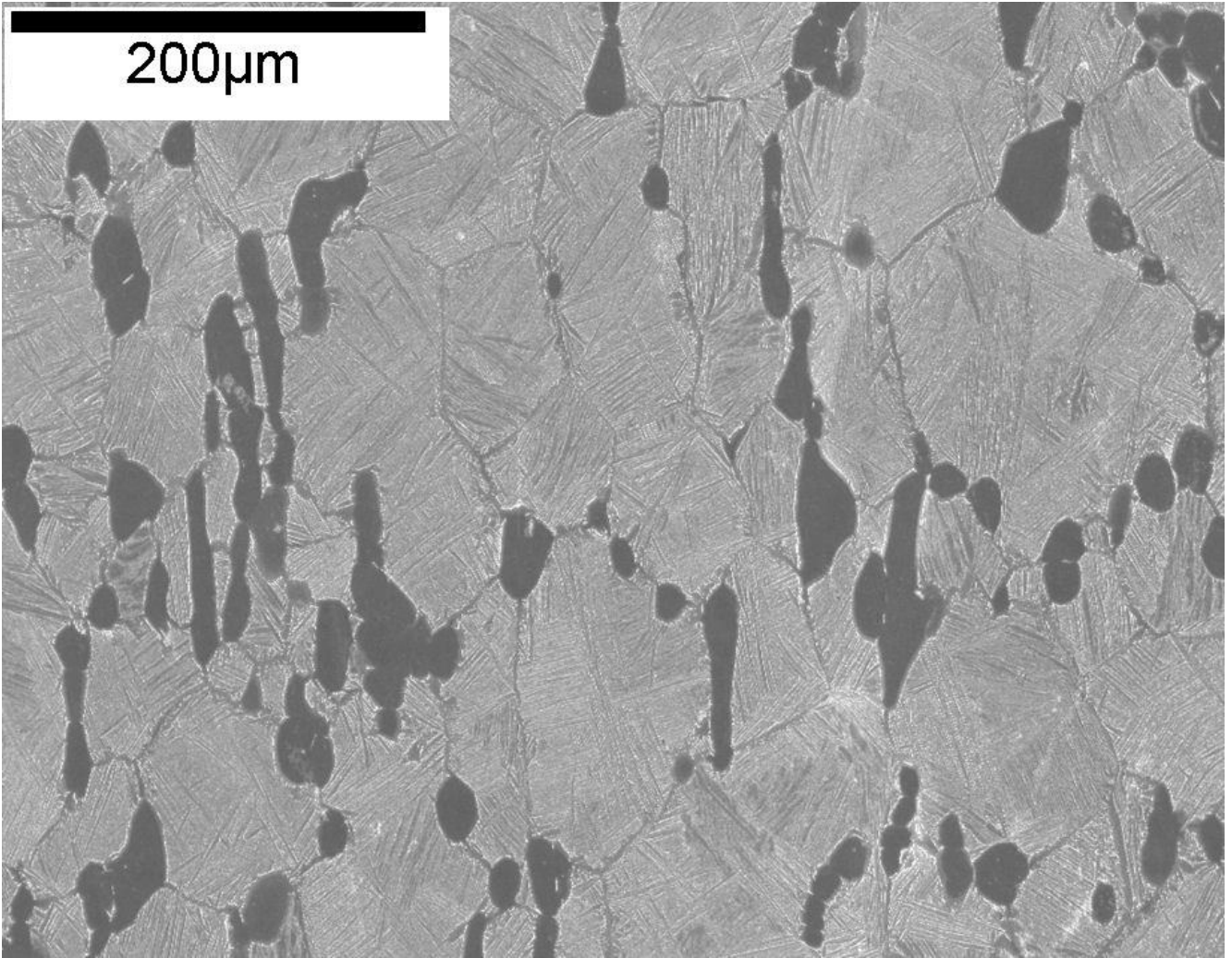


Figure 1: Microstructure of Ti834, showing a bimodal structure with a primary alpha grain size of 20-200 μm .

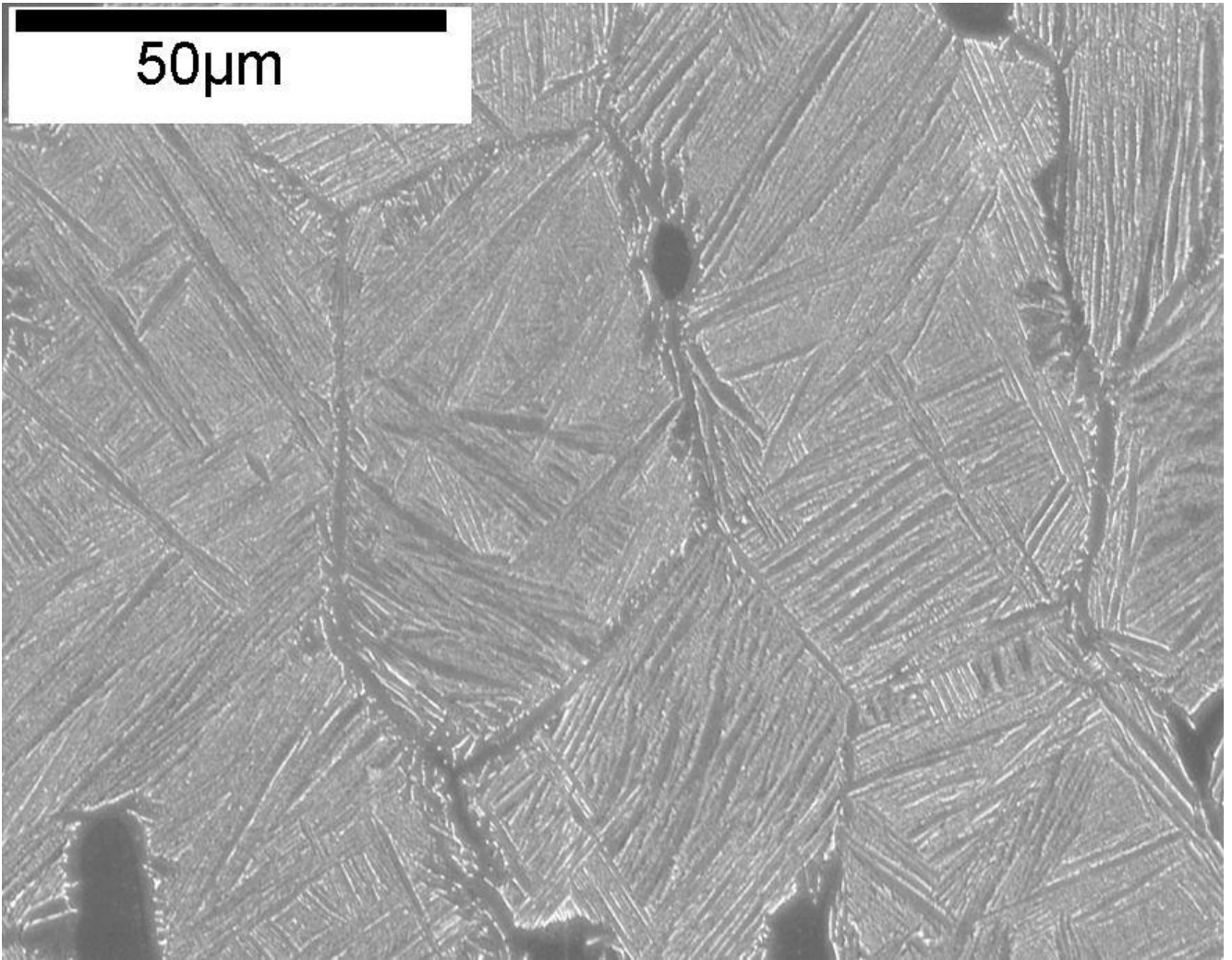


Figure 2: High magnification microstructure of Ti834, indicating Widmanstätten laths of 2-5µm thickness.

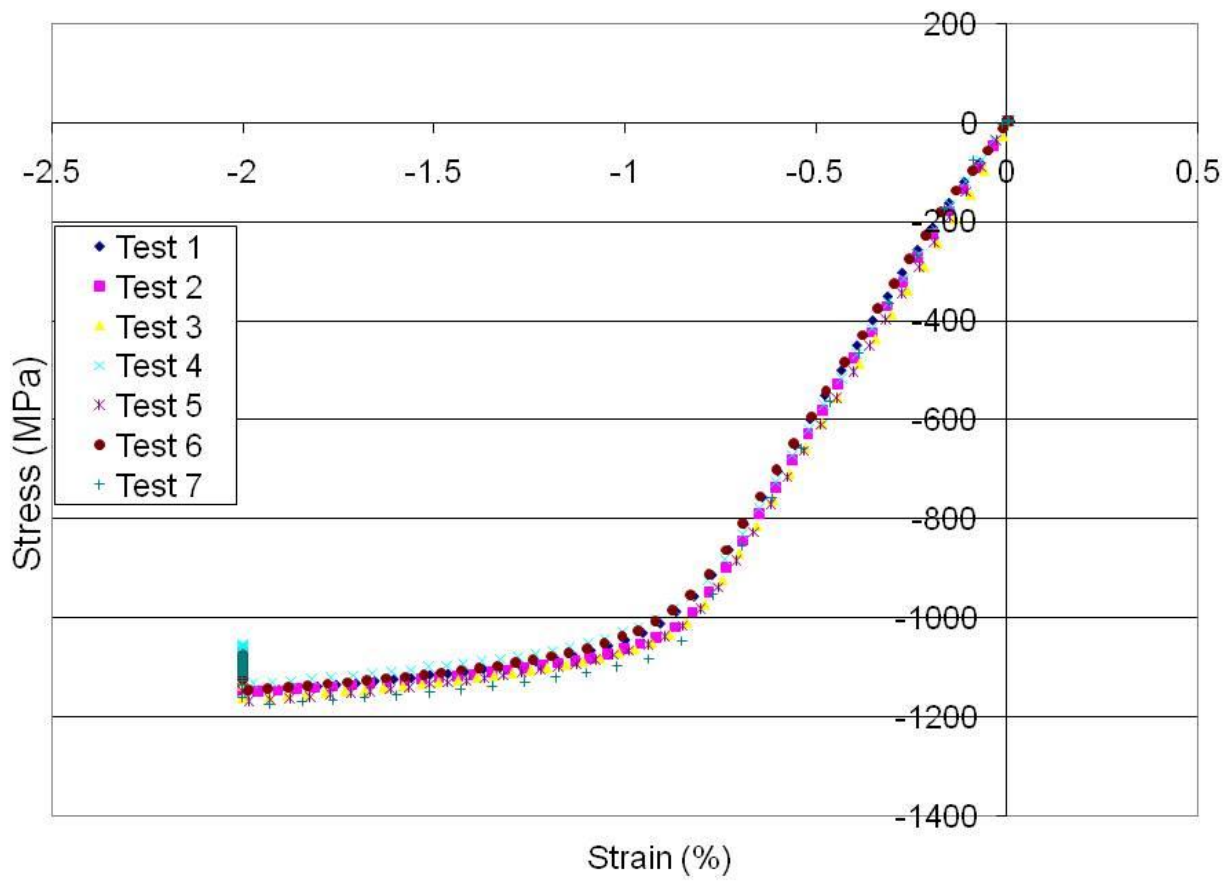


Figure 3: Stress-strain curve showing prestrain loading of -2% specimens at 20°C.

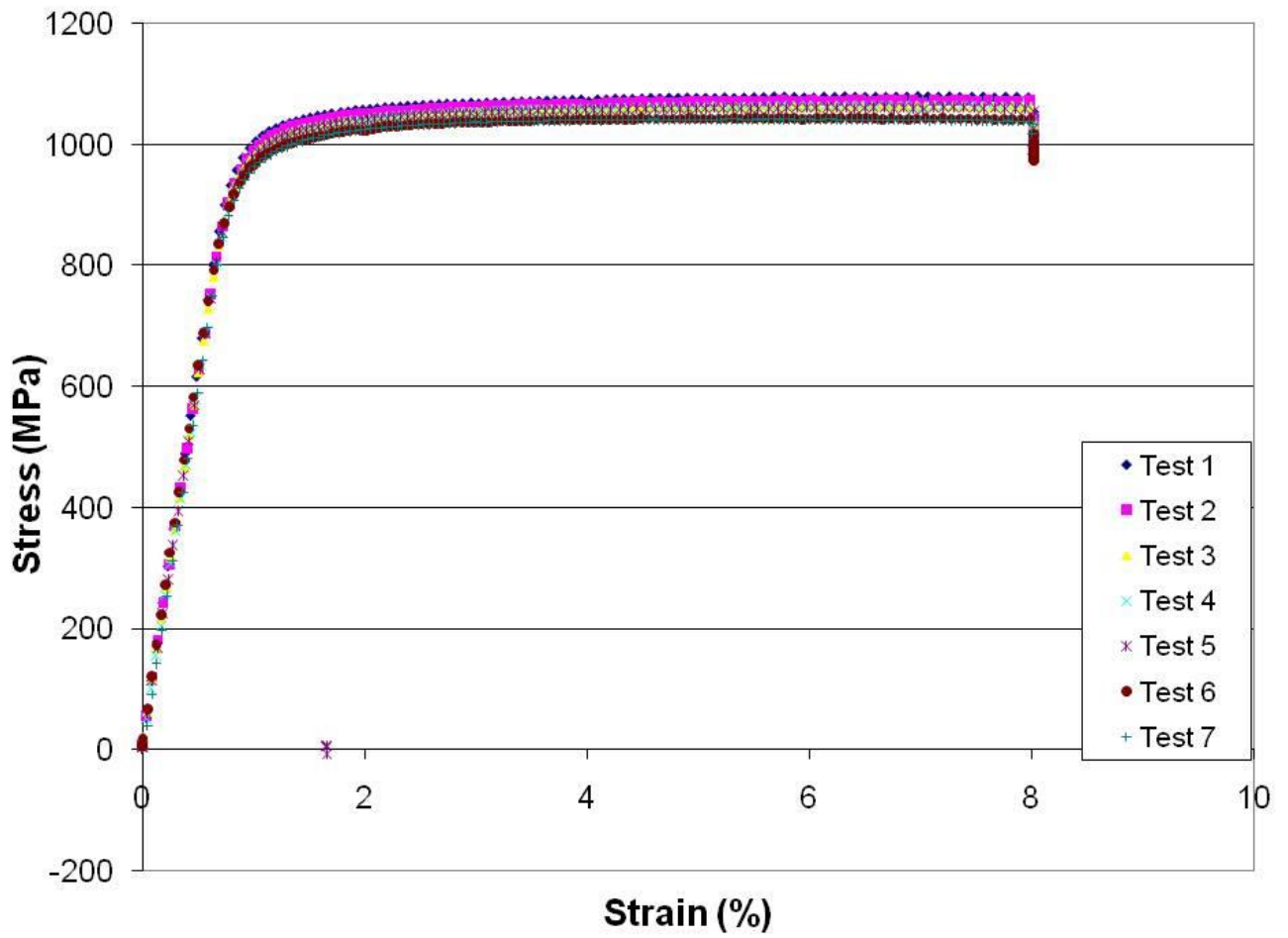


Figure 4: Stress-strain curve showing prestrain of 8% specimens at 20°C.

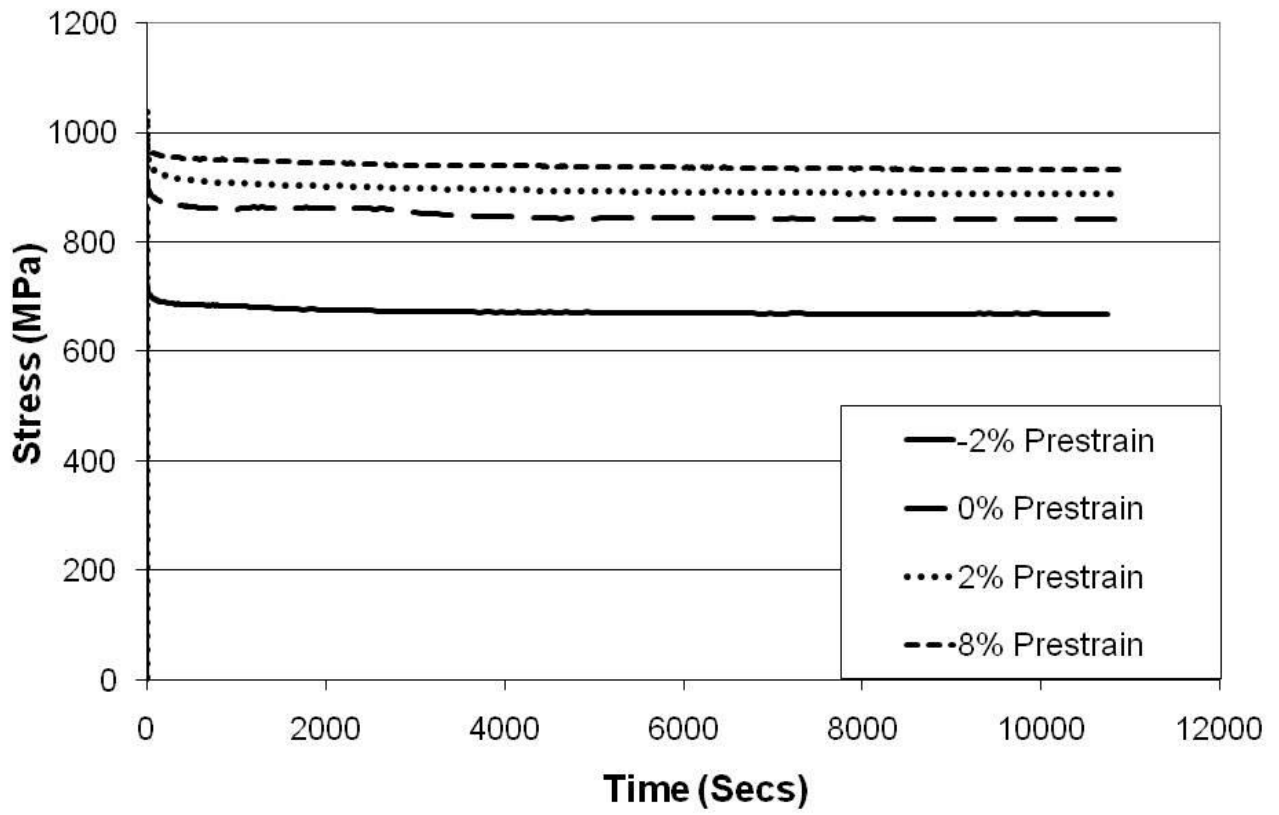


Figure 5: Comparison of stress relaxation curves of -2%, 0%, 2% and 8% specimens at 20°C.

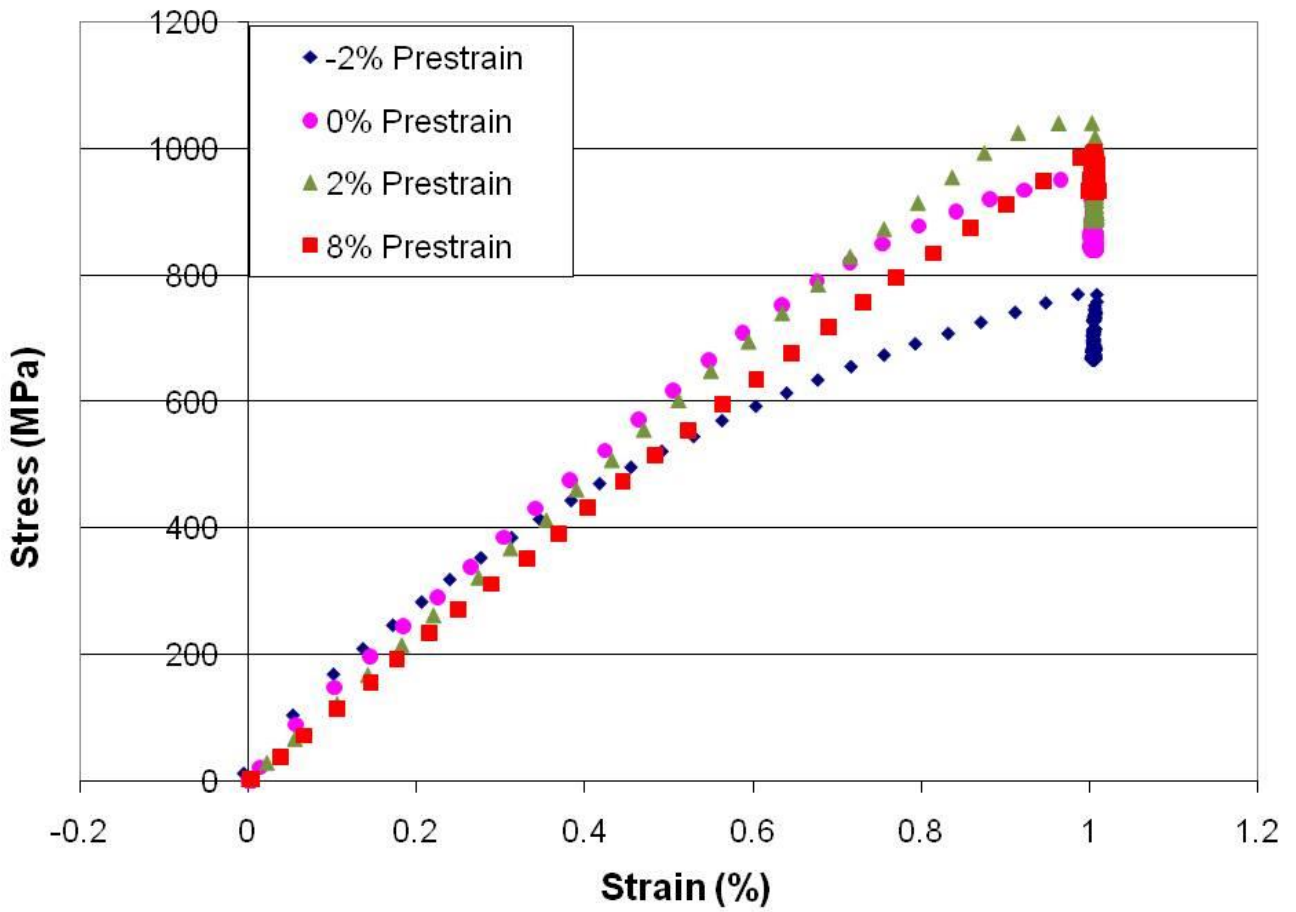


Figure 6: Loading curves for relaxation tests at 20°C indicating strain hardening in 2% and 8% specimens, and a significantly reduced yield in the -2% specimen.

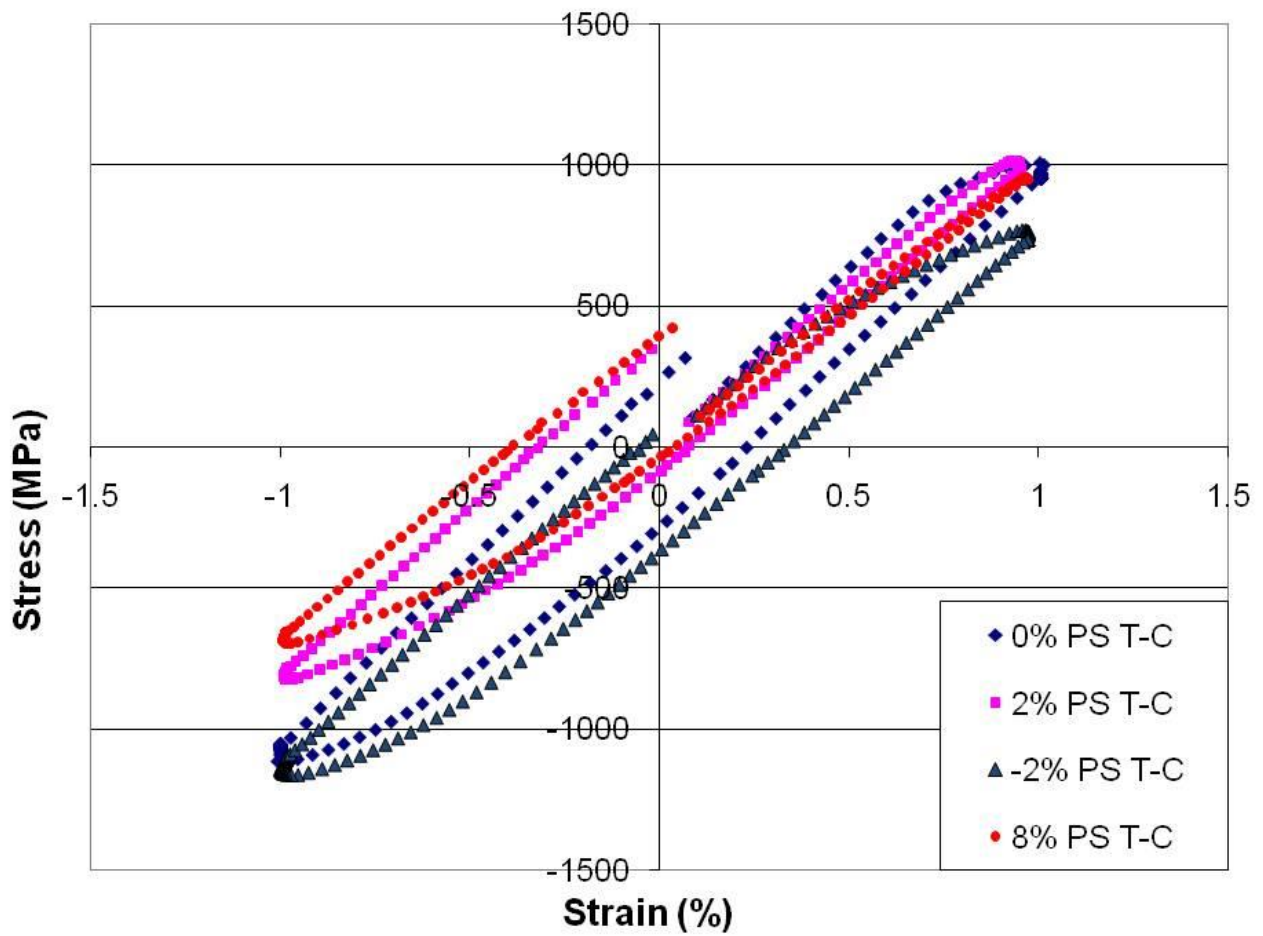


Figure 7: Comparison of initial loops of R=-1 strain control tests at 20°C, with the tensile portion of the cycle applied first (T-C).

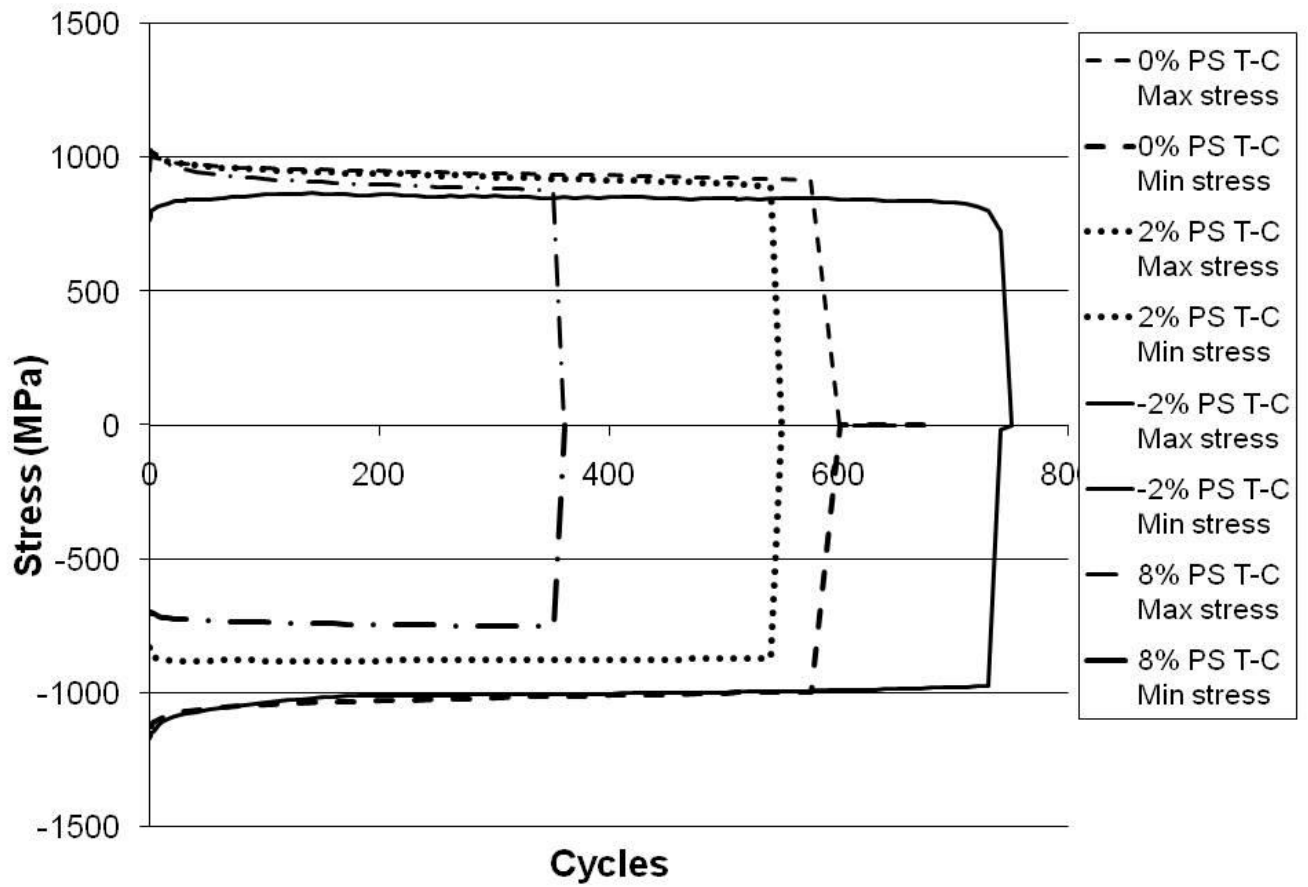


Figure 8: Evolution of maximum and minimum strains in T-C strain control tests at 20°C, indicating varying final values of minimum stress.

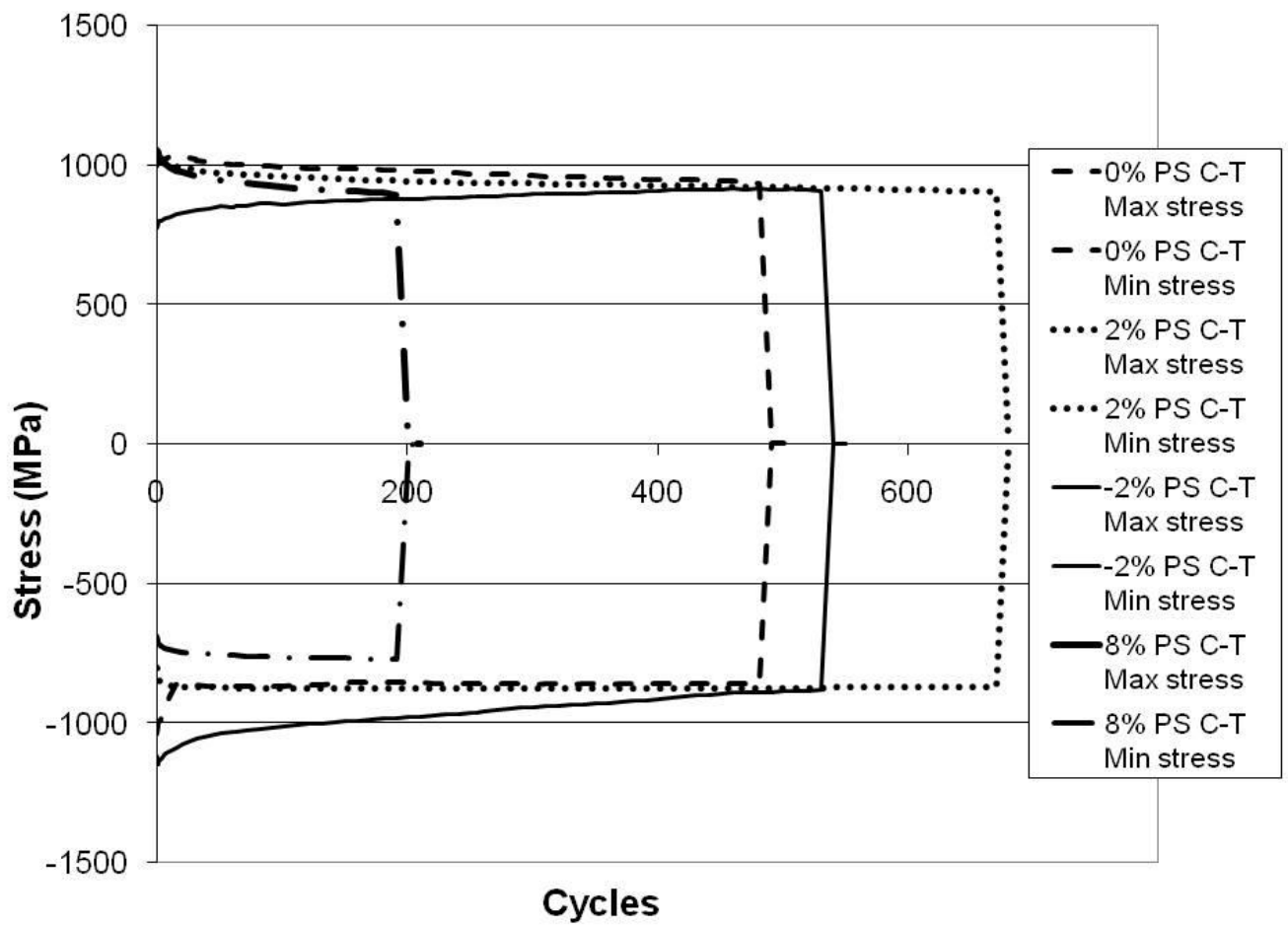


Figure 9: Evolution of maximum and minimum strains in C-T strain control tests at 20°C, showing common final values across prestrain range, except for the 8% test.

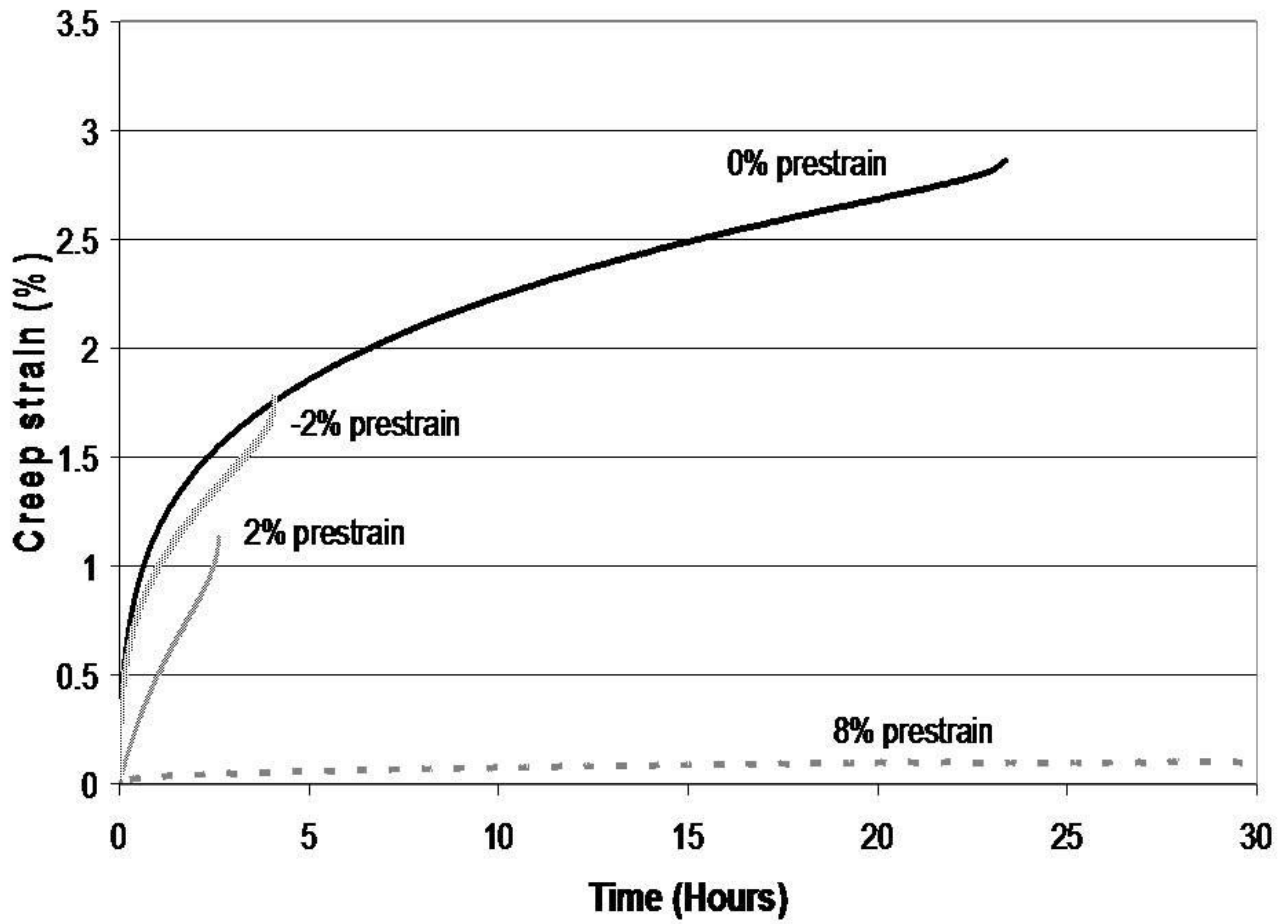


Figure 10: Creep rates of different prestrain tests at 20°C. Reduced strains to failure are seen in the -2% and 2% tests, with a significantly reduced creep rate evident in the 8% test.

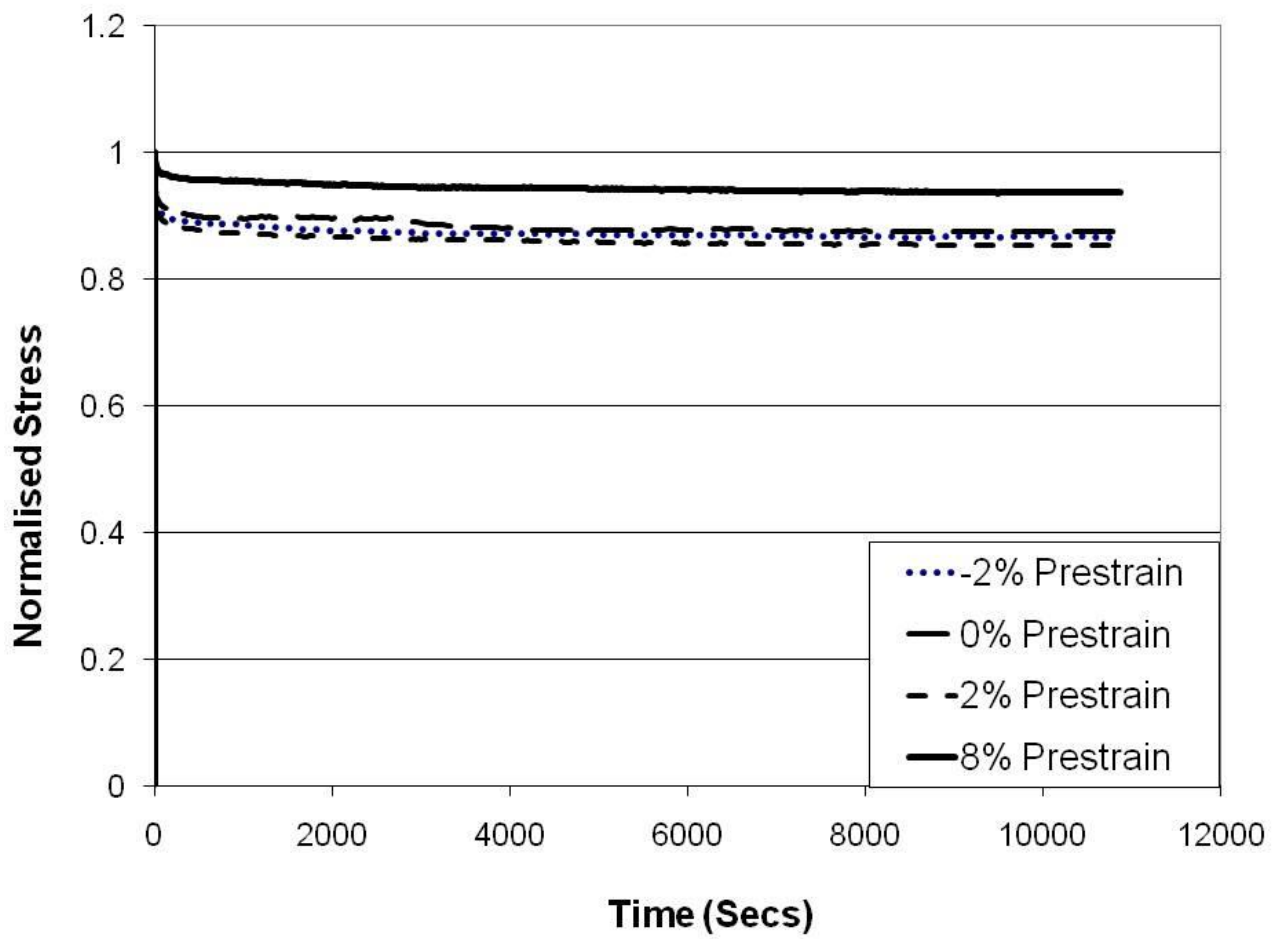


Figure 11: Normalization of stress relaxation tests by peak loading stress at 20°C.

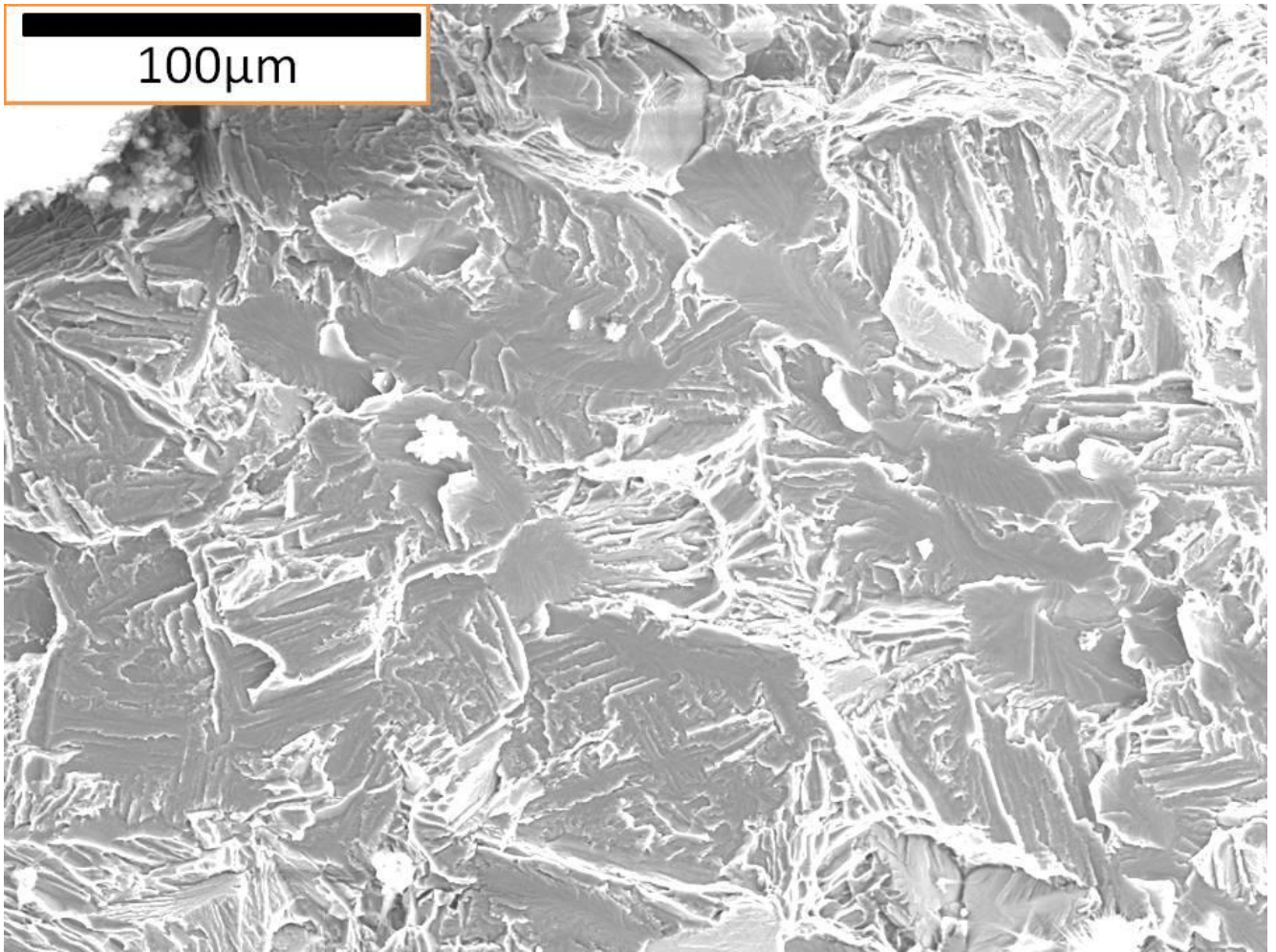


Figure 12: Cleavage of primary alpha grains and transformed product in 0% creep specimen due to consistently high applied stress values.

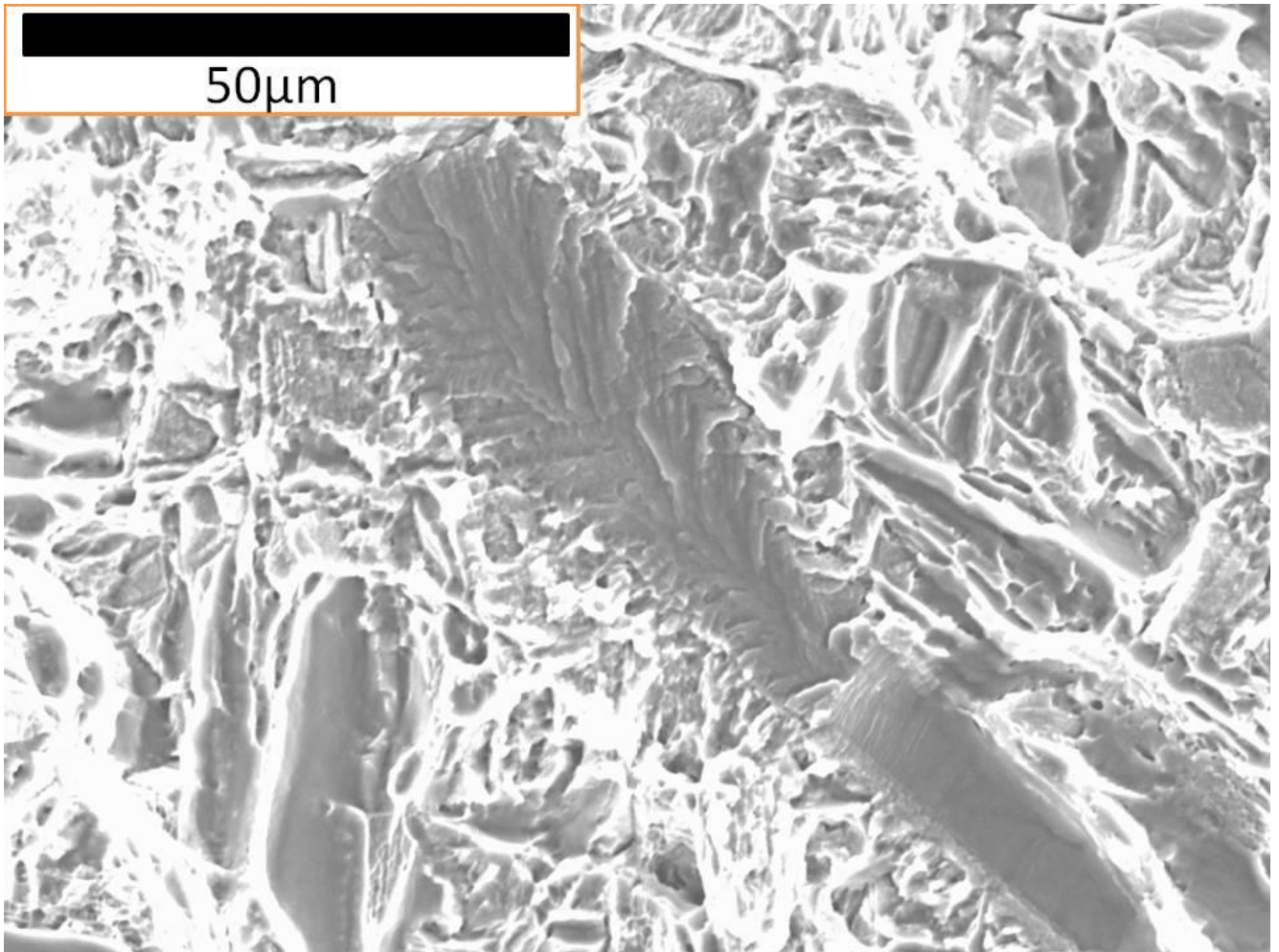


Figure 13: More isolated facets occur under stress relaxation due to the reducing stress field. Example shown is 0% prestrain specimen.

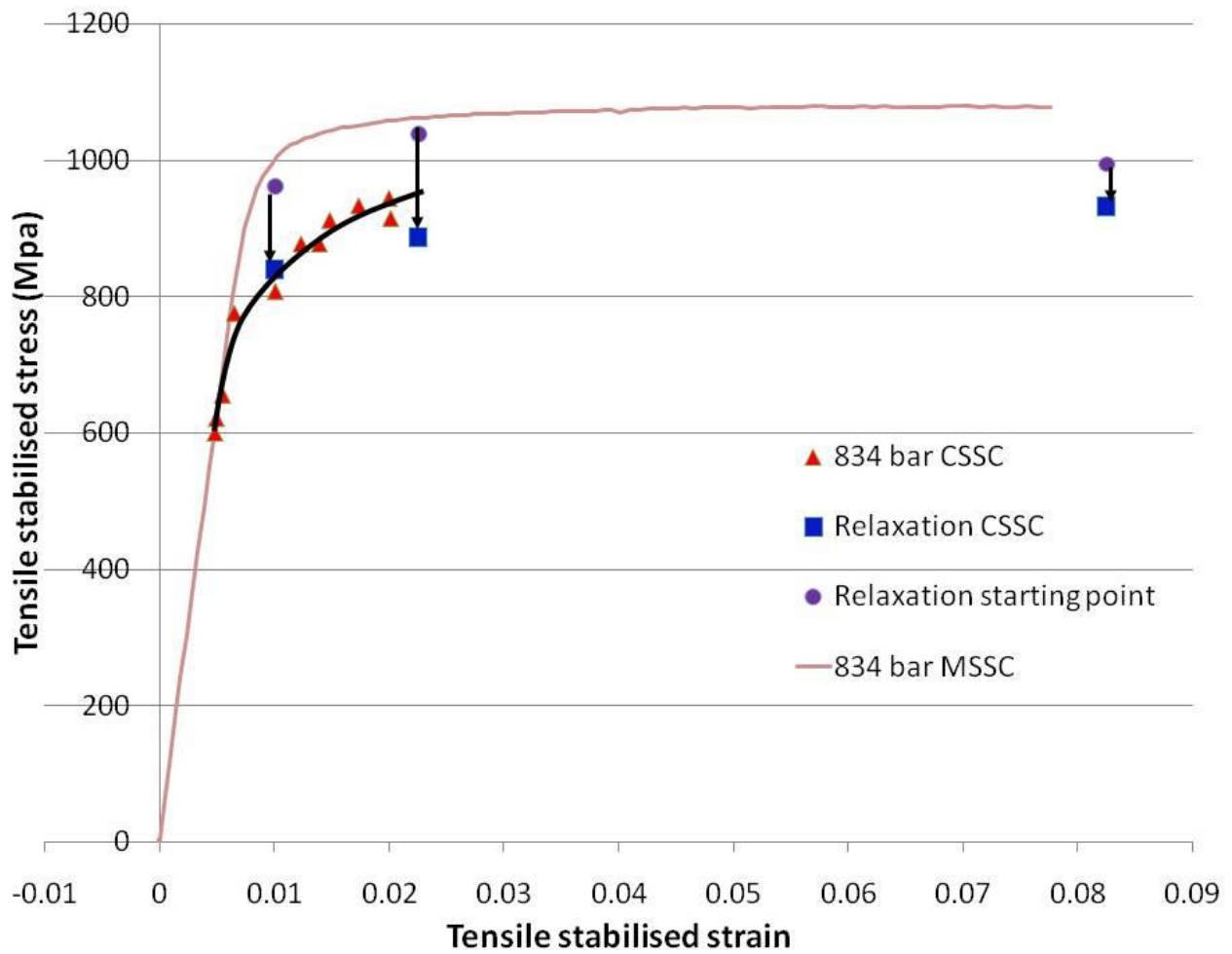


Figure 14: Association of relaxation tests with cyclic stress strain curve at 20°C, indicating the possibility that cyclic relaxation may be a result of time dependent effects.

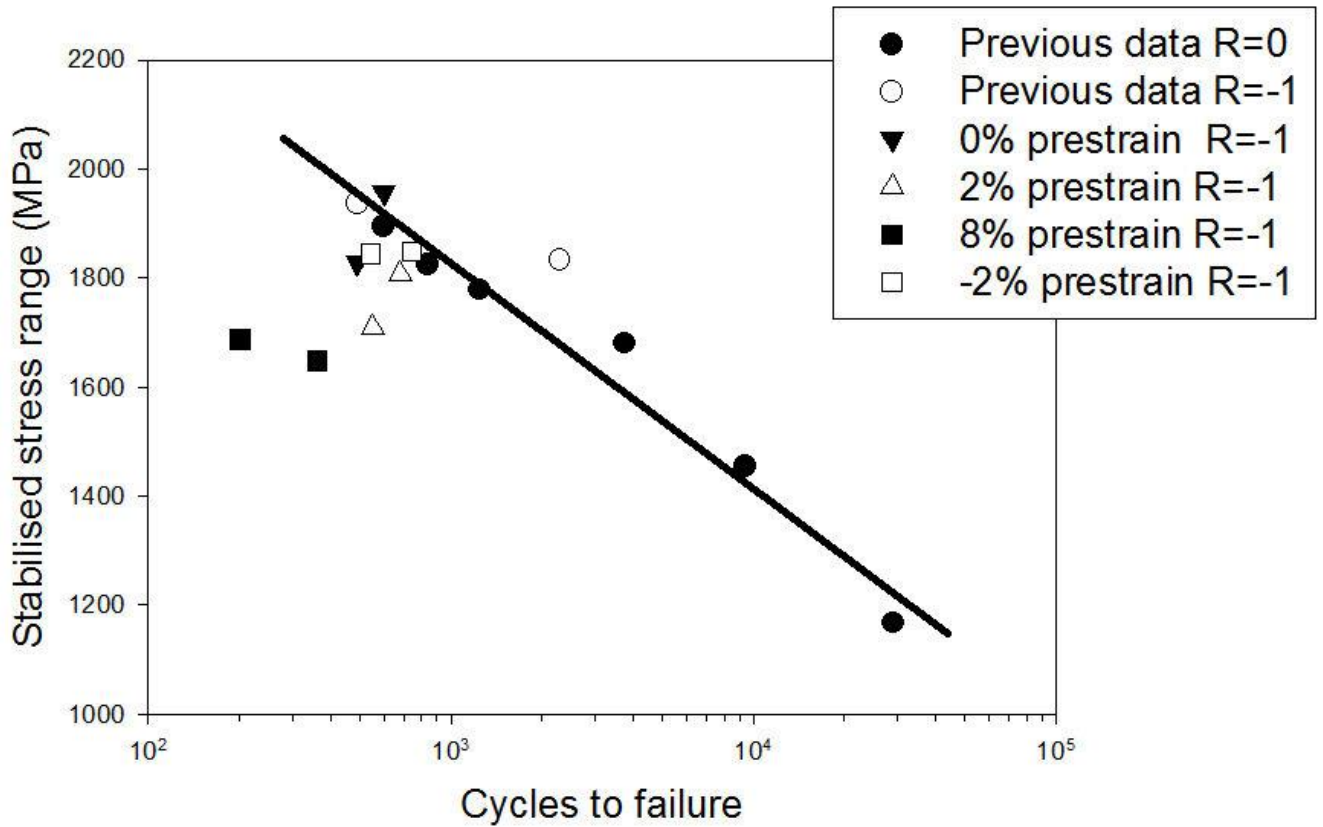


Figure 15: Fatigue lives of prestrained specimens compared with previous data^[12] at 20°C, showing a marked reduction in fatigue life for 8% specimens. Figure 14: Association of relaxation tests with cyclic stress strain curve at 20°C, indicating the possibility that cyclic relaxation may be a result of time dependent effects.

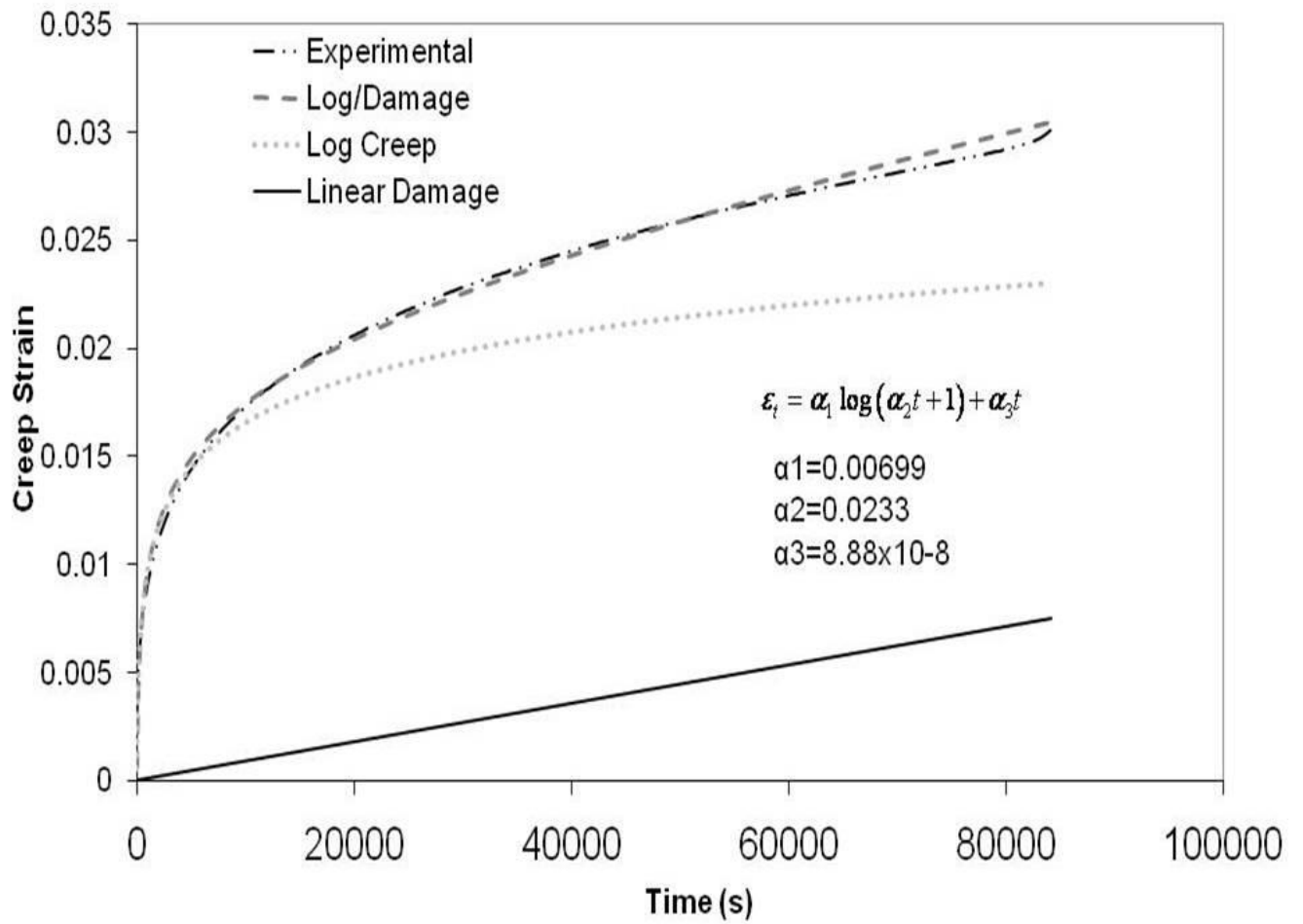


Figure 16: Modelling the evolution of creep strain in Ti834 at 20°C, using a summation of linear and logarithmic damage.